PERGAMON

Acta mater. 48 (2000) 863–874

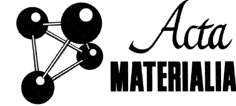

www.elsevier.com/locate/actamat

A THERMODYNAMICS MODEL FOR SOLDER PROFILE EVOLUTION

Y. X. GAO, H. FAN† and Z. XIAO

School of Mechanical and Production Engineering, Nanyang Technological University, Singapore 639798, Republic of Singapore

(Received 14 June 1999; accepted 12 October 1999)

Abstract—A thermodynamics model for describing the solder profile evolution and the triple point line motion driven by surface tensions and gravity field is proposed. Attention is focused on the kinetic process as the solder profile evolves toward its equilibrium shape in its molten state. Based upon non-equilibrium thermodynamics, a theoretical model is proposed by introducing the kinetic laws that characterize the motions of the solder surface and the triple point line. The presented model leads to a nonlinear dynamic system, which describes the entire time-dependent process of the solder wetting. It can be applied not only to predict the equilibrium shape of the solder, but also the shape at any time during the spreading process. A computer numerical simulation and examples for the solution of the dynamic system are described. © *2000 Acta Metallurgica Inc. Published by Elsevier Science Ltd. All rights reserved.*

Keywords: Solder wetting; Computer simulation; Surfaces & interfaces; Kinetics; Theory & modeling

1. INTRODUCTION

As the density of interconnects and conductor lines in electronic packages is increasing and the size of microelectronic devices is decreasing rapidly, the capability of soldering must be improved. Improving solder processes to meet the rapidly changing design requirements in electronic packaging is a great challenge to the engineers who are supporting solder processes and the researchers who are trying to understand the fundamental physical laws involved in the solder process and thus to describe the solder process quantitatively. The logical steps in improving solder processes are to develop models that can predict the solder process in terms of a set of packaging design parameters, and conversely, using the models to optimize these parameters in order to yield reliable electronic devices. Therefore, the advancements in the modeling and simulation of the process of soldering are as important as the development of solder assembly processes themselves.

In recent years, many researchers have developed various theoretical models for predicting solder geometry in electronic packaging. One of the important reasons to predict the solder geometry is that wetting balance tests in the electronic packaging industry are related to molten solder geometries and the corresponding forces [1, 2]. Heinrich and Lee [3] presented an exhaustive literature survey on solder geometry modeling. It is noted that all of the solder geometry models can only predict the static equilibrium shape of the solder in its molten state, because the models are based on the static surface tension theory [4]. There are several additional contributions in this area dated after Heinrich and Lee's survey [3]. Li and Mahajan [5] presented a model to predict the eutectic solder fillet shape for a ceramic ball grid array joint. Chiang and Chen [6] gave an efficient numerical method and compared their results with the Surface Evolver program [7] to discuss the influences of the geometric parameters. Renken and Subbarayan [8] presented a general two-body formulation for solder joint shape prediction. All the above-mentioned results were also based on the static surface tension theory and therefore cannot account for kinetic and dynamic effects in the process of solder wetting and spreading.

It is well known that the solder process, such as wetting and spreading, is not a static equilibrium state process. Experiments [9] showed that when a solder droplet is placed on a wettable solid surface, it first experiences an extremely rapid spreading before it reaches the static equilibrium shape. The overview of the results by using Surface Evolver to simulate the behavior of molten solders in wetting balance tests [10] showed that some of the empirical

† To whom all correspondence should be addressed.

1359-6454/00/$20.00 © 2000 Acta Metallurgica Inc. Published by Elsevier Science Ltd. All rights reserved.
PII: S1359-6454(99)00381-X

observations cannot be fully explained by a static surface tension model. Moon *et al.* [11] also discussed the dynamic aspects of wetting balance tests. They pointed out that the time-dependent contact angle is an important quantity because the changing rate of the contact angle must be fast enough to respond to wave soldering travel rates or to solder paste reflow rates. Since the static equilibrium models cannot describe the time-dependent phenomenon, such as the time duration for a solder droplet to evolve from a given initial state to its static equilibrium shape, it is essential to develop kinetic models for understanding the solder evolution processes.

Nevertheless, solder with its environment in electronic packaging is a complex system, which involves multiple thermodynamic processes and chemical change [12]. Solving this general system completely is quite formidable. In scientific inquiry, when we are interested in understanding or predicting some complex phenomenon, we use the technique of modeling. Thus, regardless of the complexity, our modeling is focused on elementary processes so as to understand fundamental physical principles in the processes of solder wetting and spreading. Boettinger *et al.* [13] showed the complex physical processes involved in the spreading of molten solder and surveyed the previous attempts to model the kinetic process. For instance, Ehrhard and Davis [14] modeled the solder wetting process using fluid mechanics and Aksay *et al.* [15] proposed an approach to coupling the reaction to the contact line motion. It is noticed that an assumed relation between the triple point line (TPL) motion and current contact angle was normally adopted in these analyses. Unfortunately, these "constitutive relations" had been constantly questioned by experimental observations [11, 13]. As discussed in Section 6, the present thermodynamics model is able to derive the so-called constitutive relation (between the TPL motion and contact angle) from the kinetic laws of the non-equilibrium thermodynamic system.

The aim of some of the recent works [16–23] was to understand the complex wetting process. Mortensen *et al.* [16, 17] and Voitovitch *et al.* [18] examined the kinetics of diffusion-limited reactive wetting and discussed the dependence of the solder drop spreading rate on the diffusion of the reactive atom species from the bulk liquid to the solid–liquid–vapor triple point line. They focused on modifying the above-mentioned "constitutive relations" by considering reactive wetting. Based upon the wetting kinetics suggested by Wang and Lannutti [19], Yost *et al.* [20] discussed the energetics and kinetics of the dissolutive wetting process and described the thermodynamic equilibrium conditions and the wetting kinetic equations by using the concepts of entropy production. However, these kinetic laws written in the manner of Onsager rate equations can be applied only to the processes nearby the equilibrium states. In addition, the solder liquid profile was assumed to be a spherical cap during spreading in their analysis. Warren *et al.* [21] modeled the situation in which local equilibrium had been established at the liquid–solid interface and transport of solute occurs by diffusion coupled to a simple model of fluid flow. Their model was only applicable to the stages of wetting after the fluid flow had created a spherical cap. The aim of both Refs [20, 21] was to understand reactive wetting. Nevertheless, the geometric complexity of solder profile change in the solder wetting process has not been fully understood up to now. Even the simplest case of a droplet of liquid solder material spreading on a smooth and horizontal substrate without dissolution and reaction between the solder liquid and the substrate materials is not well addressed. Therefore, it is the objective of the present study to describe the entire time-dependent spreading process from any initial state (far from the equilibrium state) to the final equilibrium state and the evolution of solder liquid surface shape during this process.

Following the thermodynamic framework of dynamic systems, this paper presents a new model focused on the kinetic process that the solder profile evolves toward the static equilibrium shape in its molten state. We propose a theoretical model for describing the process of molten solder profile evolution and triple point line motion in terms of the global approach to the motions of the microscopic surface in materials [24, 25]. The model aims to describe the entire process of the molten solder's kinetic evolution, not only to predict the equilibrium shape of the solder, but also to record the whole history of the spreading process.

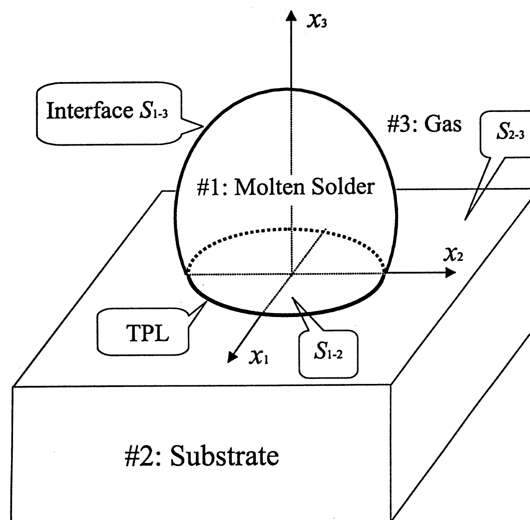

Fig. 1. A molten solder spreading on a substrate.

2. NON-EQUILIBRIUM THERMODYNAMIC PROCESS

The model presented in this paper is based on the framework of non-equilibrium thermodynamics [24, 25]. Consider a droplet of liquid solder material, spreading on a smooth and horizontal substrate, illustrated in Fig. 1. It is assumed that the substrate does not dissolve or otherwise react with the droplet. When a small droplet of liquid solder material is placed on the surface of a substrate, it first experiences an extremely rapid spreading and then is followed by a slow spreading. During the spreading process, the profile of the solder droplet evolves rapidly at first, then slows down, and finally reaches a static equilibrium shape in its molten state by the solidification process. Many ingredients such as free energy, driving forces and kinetic laws of a non-equilibrium thermodynamic system are considered in this section to establish the thermodynamics model for the solder profile evolution.

2.1. Free energy

The solder profile evolution toward an equilibrium state is driven by the change of free energy, denoted by G hereafter. Generally, the free energy of a system consists of internal energy U and potential energy Π, namely

$$G = U + \Pi. \tag{1}$$

For the system considered here, the internal energy U comes from the interface energies among different materials

$$U = \gamma_{1-2}A_{1-2} + \gamma_{1-3}A_{1-3} + \gamma_{2-3}A_{2-3} \tag{2}$$

where γ_{i-j} is the specific surface tension and A_{i-j} is the area of the interface S_{i-j} between material i and material j, with materials 1, 2 and 3 denoting the liquid of solder, the solid of substrate and the gas surrounding the solder, respectively, as shown in Fig. 1. In this paper, γ_{i-j} is assumed to be isotropic. Generally, the internal energy relates to the global quantities, such as volumes and areas, of the system. On the other hand, the potential energy considered in this section is the negative work supply W to the system by the external actions of the system

$$\Pi = -W. \tag{3}$$

Thermodynamics requires that evolutions proceed to decrease the free energy of the system.

2.2. Motion of solder surface and triple point line

Free energy by itself is insufficient to determine the shape change of the solder profile, because countless ways of shape change would reduce the free energy. To obtain the solder profile shape, the model needs more ingredients.

Figure 2 illustrates the motion of the interface S_{1-3} between the liquid and the gas, and the motion of the triple point line (TPL) at the junction of the liquid, the solid and the gas. A virtual motion of the interface is a small movement in the direction normal to the interface that need not obey any kinetic law. The magnitude of the virtual motion, δr_n, can differ from point to point over the interface. Similarly, a virtual motion of the TPL is a small movement in the direction normal to the TPL in the plane of the substrate surface that also need not obey any kinetic law. The magnitude of the virtual motion of the TPL denoted by $\delta r_n^{(t)}$ can differ from point to point along the TPL.

Since the surface tension is assumed to be isotropic, the liquid–gas interface at a given time is usually a smooth curved surface. The area of a surface element is denoted by dA, the length of a line element by dl and the unit vector normal to the surface by $\mathbf{n}$, taken to direct the gas phase. Of particular interest is the sum of the two principal curvatures

$$\kappa = \frac{1}{R_1} + \frac{1}{R_2} \tag{4}$$

where R_1 and R_2 are the principal radii of curvature, taken to be positive for a convex surface. Associated with the virtual motion, δr_n, the area of the interface S_{1-3} varies by

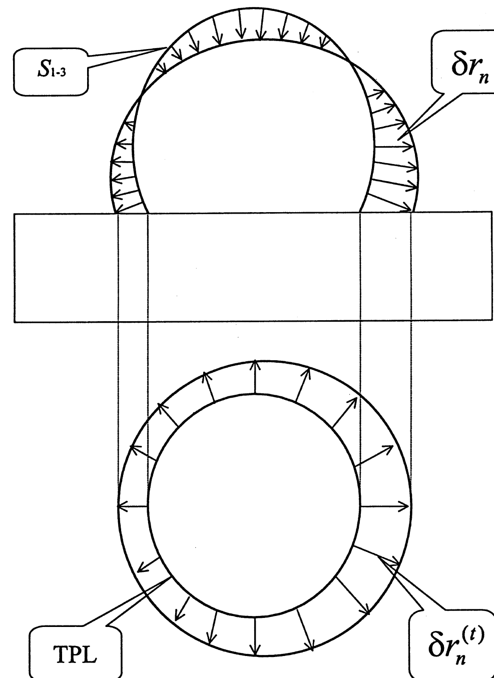

Fig. 2. The interface S_{1-3} or the TPL undergoes a virtual motion δr_n or $\delta r_n^{(t)}$.

$$\delta A_{1-3} = \iint_{S_{1-3}} \kappa \delta r_n \, dA \tag{5}$$

and the volume of the solder varies by

$$\delta V = \iint_{S_{1-3}} \delta r_n \, dA. \tag{6}$$

The integrals extend over the interface S_{1-3}.

Similarly, associated with the virtual motion of the TPL, $\delta r_n^{(t)}$, the area of the interface S_{1-2} varies by

$$\delta A_{1-2} = \oint_{L_t} \delta r_n^{(t)} \, dl \tag{7}$$

and the area of the interface S_{2-3} varies by $-\delta A_{1-2}$. The integral extends along the TPL, denoted by L_t.

During the process of solder spreading, it is noted that the virtual motions at any point on the TPL at any time must be satisfied with the following contact condition:

$$\delta r_n = \delta r_n^{(t)} \sin \theta, \quad \text{on } L_t \tag{8}$$

where θ is the current contact angle at any point on the TPL. Of course, the volume of the solder remains unchanged, namely

$$\delta V = 0. \tag{9}$$

The contact condition (8) and the constrained condition (9) will be fulfilled in our numerical procedure (Section 5).

2.3. Driving forces and kinetic laws

Associated with the virtual motions, the free energy of the system varies by δG. Define the thermodynamic force on the interface, f, that drives the interface motion and the force on the TPL, f_t, that drives the TPL motion, as the free energy decreases with respect to the virtual motions

$$\oint_{L_t} f_t \delta r_n^{(t)} \, dl + \iint_{S_{1-3}} f \delta r_n \, dA = -\delta G. \tag{10}$$

Since the virtual motion δr_n is an arbitrary function of the position on the interface S_{1-3} and $\delta r_n^{(t)}$ is also an arbitrary function of the position on the line L_t, equation (10) uniquely defines the quantity f at every point on the interface S_{1-3} and the f_t at every point on the TPL L_t. The above-defined thermodynamic force f has a unit of stress (force/area) and f_t has a unit of surface tension (force/length), they are called driving forces of the dynamic system.

Let v_n and $v_n^{(t)}$ be the actual velocity of the interface S_{1-3} and the TPL L_t, respectively. Following the framework of the dynamic system, the actual velocities are taken to be functions of the driving forces. Specifically, the velocity is assumed to be linearly proportional to the driving force as

$$v_n^{(t)} = M_t f_t \tag{11a}$$

$$v_n = M f. \tag{11b}$$

Here M_t and M are called the mobility of the TPL and the interface, respectively. These two quantities are important for the system of solder profile evolutions. They will be used as phenomenological parameters of the model, to be determined by comparing model predictions with experimental observations. Since thermodynamics requires that the solder surface move in the direction that reduces the free energy of the system, both M_t and M are positive. Equations (11a) and (11b) are the so-called kinetic laws for the TPL and the interface. Here it should be noted that the kinetic laws applied in this paper are linear relations and the velocity at a point only depends on the force at this point, namely, the kinetic laws are also local relations. For a more universal system, the kinetic laws may be extended to nonlinear and nonlocal relations. However, at the first stage, it is assumed that both M_t and M are uniform and isotropic, they are thus material constants for the kinetic model in the present analysis.

The free energy, motion descriptions, driving forces and kinetic laws discussed above define the dynamics of solder wetting and spreading. At a given time, the variation of the free energy of the system determines the driving forces first, then the kinetic laws update the solder profile shape for a small time step. The process repeats for many time steps to evolve the solder profile shape up to the equilibrium shape.

3. MOTION EQUATIONS AND EQUILIBRIUM CONDITIONS

From equations (1), (2) and (3), the free energy change of the solder evolution system can be expressed by

$$\begin{aligned} \delta G = {} & \gamma_{1-2} \delta A_{1-2} + \gamma_{1-3} \delta A_{1-3} \\ & + \gamma_{2-3} \delta A_{2-3} - \delta W. \end{aligned} \tag{12}$$

When the interface S_{1-3} moves by virtual motion δr_n and the TPL, L_t, moves by $\delta r_n^{(t)}$, the areas of interfaces S_{1-2} and S_{2-3} change by

$$\delta A_{1-2} = \oint_{L_t} \delta r_n^{(t)} \, dl$$

and $\delta A_{2-3} = -\delta A_{1-2}$, respectively, and the area of S_{1-3} changes by

$$\delta A_{1-3} = \oint_{L_t} \delta \, r_n^{(t)} \cos \theta \, dl + \iint_{S_{1-3}} \kappa \delta r_n \, dA.$$

Associated with the virtual motions, the external work changes by

$$\delta W = \iint_{S_{1-3}} \Delta p \delta r_n \, \mathrm{d}A$$

where Δp is the pressure difference across the surface S_{1-3}. Consequently, associated with the virtual motions of the TPL and the interface, the free energy changes by

$$\delta G = \oint_{L_t} \gamma_{1-2} \delta r_n^{(t)} \, \mathrm{d}l - \oint_{L_t} \gamma_{2-3} \delta r_n^{(t)} \, \mathrm{d}l + \oint_{L_t} \gamma_{1-3} \delta r_n^{(t)} \cos\theta \, \mathrm{d}l + \iint_{S_{1-3}} \gamma_{1-3} \kappa \delta r_n \, \mathrm{d}A - \iint_{S_{1-3}} \Delta p \delta r_n \, \mathrm{d}A. \quad (13)$$

A comparison of equations (10) and (13) gives the expressions for the driving forces:

$$f_t = \gamma_{2-3} - \gamma_{1-2} - \gamma_{1-3} \cos\theta \quad (14a)$$

$$f = \Delta p - \kappa \gamma_{1-3}. \quad (14b)$$

Equation (14a) expresses the driving force on the TPL in terms of the current contact angle θ, and surface tension, γ_{i-j}. It has the clear physical significance that f_t is the sum of the surface tensions projected along the unit vector normal to the TPL in the surface of the substrate. Equation (14b) expresses the driving force on the interface in terms of the current curvature κ, and the external action, Δp, as well as the surface tension, γ_{1-3}. As expected, the surface tension, γ_{1-3}, tends to drive the solder surface in the direction toward the center of curvature.

A combination of equations (11) and (14) leads to

$$v_n^{(t)} = M_t(\gamma_{2-3} - \gamma_{1-2} - \gamma_{1-3} \cos\theta) \quad (15a)$$

$$v_n = M(\Delta p - \kappa \gamma_{1-3}). \quad (15b)$$

These partial differential equations govern the motions of the TPL and the surface of the liquid solder droplet during the solder spreading process. The process of solder profile evolution depends on the solution of the set of motion equations (15) under the contact condition (8), volume constraint (9) and certain initial-value and boundary conditions.

Moreover, at the end of the evolution process of the solder profile, the solder droplet will arrive at a static equilibrium state. At that time, the free energy of the system attains the minimum value, the solder profile remains unchanged, and the driving forces vanish. Setting $f_t = 0$ and $f = 0$ in equations (14) results in the equilibrium conditions for the TPL and the interface as

$$\gamma_{2-3} - \gamma_{1-2} - \gamma_{1-3} \cos\theta_e = 0 \quad (16a)$$

$$\Delta p - \kappa_e \gamma_{1-3} = 0 \quad (16b)$$

where θ_e and κ_e are the contact angle and the curvature in the equilibrium state, respectively. Equations (16a) and (16b) are the well-known Laplace–Young equations. They are frequently applied to predict the solder geometry in static equilibrium states [3].

4. WEAK STATEMENT AND GENERALIZED COORDINATES

It is quite formidable to solve the set of partial differential equations (15) in addition to certain specific conditions because of their nonlinear features. Following Suo [24], the nonlinear dynamic system is formulated by a weak statement. This scheme has been successfully used in modeling many non-equilibrium problems [24, 25]. Even for more complicated cases, say, γ_{i-j} are anisotropic, the weak statement can be applied without extra difficulties.

Replacing the driving forces, f_t and f, in equation (10) with the velocities, $v_n^{(t)}$ and v_n, of the TPL and the interface by using the kinetic laws (11), gives

$$\oint_{L_t} \frac{v_n^{(t)}}{M_t} \delta r_n^{(t)} \, \mathrm{d}l + \iint_{S_{1-3}} \frac{v_n}{M} \delta r_n \, \mathrm{d}A = -\delta G. \quad (17)$$

This is the so-called weak statement for the dynamic system. It means that the actual velocities, $v_n^{(t)}$ and v_n, must satisfy equation (17) for any of the arbitrary distributions of virtual motions, $\delta r_n^{(t)}$ and δr_n, on the TPL and the interface S_{1-3}, respectively. The weak statement is equivalent to the virtual work principle commonly studied in dynamics. Both of them lead to the Galerkin method in numerical simulation.

Let both the solder surface, S_{1-3}, and the TPL, L_t, be described by m generalized coordinates, $\mathbf{q} = \{q_1, q_2, \ldots, q_m\}$, and the corresponding generalized velocities, $\dot{\mathbf{q}} = \{\dot{q}_1, \dot{q}_2, \ldots, \dot{q}_m\}$. Based on the differential geometry, the evolving surface S_{1-3} can be expressed by the position vector on the surface, $\mathbf{x} = \mathbf{x}(t)$, at a given time, then the position vector can be expressed as $\mathbf{x} = \mathbf{x}(q_1, q_2, \ldots, q_m)$ by the generalized coordinates with the time implicitly contained in the generalized coordinates. Similarly, the position vector, $\mathbf{x}^{(t)}$, on the TPL in the plane of the substrate surface can also express the moving TPL, namely, $\mathbf{x}^{(t)} = \mathbf{x}^{(t)}(q_1, q_2, \ldots, q_m)$. Therefore, the virtual motions, $\delta r_n^{(t)}$ and δr_n, are linear in the variations of the generalized coordinates

$$\delta r_n^{(t)} = \sum_{i=1}^{m} \left(\mathbf{n}^{(t)} \cdot \frac{\partial \mathbf{x}^{(t)}}{\partial q_i} \right) \delta q_i \equiv \sum_{i=1}^{m} N_i^{(t)} \delta q_i \quad (18a)$$

$$\delta r_n = \sum_{i=1}^{m} \left(\mathbf{n} \cdot \frac{\partial \mathbf{x}}{\partial q_i} \right) \delta q_i \equiv \sum_{i=1}^{m} N_i \delta q_i. \quad (18b)$$

Here, $N_i^{(t)}$ and N_i, the shape functions, depend on the generalized coordinates but not on the generalized velocities. Moreover, the actual velocities, $v_n^{(t)}$ and v_n, are linearly related to the generalized velocities, namely

$$v_n^{(t)} = \sum_{i=1}^{m} N_i^{(t)} \dot{q}_i, \quad v_n = \sum_{i=1}^{m} N_i \dot{q}_i. \tag{19}$$

Simultaneously, the free energy is a function of the generalized coordinates, namely, $G = G(q_1, q_2, \ldots, q_m)$. The generalized forces, $f_1, f_2, \ldots, f_m$, conjugating to the generalized coordinates, are the differential coefficients of the free energy

$$f_i = -\frac{\partial G}{\partial q_i} \tag{20}$$

and the free energy variation is

$$\delta G = \sum_{i=1}^{m} \left(\frac{\partial G}{\partial q_i} \delta q_i \right) = -\sum_{i=1}^{m} f_i \delta q_i. \tag{21}$$

Here the generalized force, f_i, can be obtained by comparing equation (21) with the result from substituting equations (18) into equation (13) as

$$f_i = \oint_{L_t} f_t N_i^{(t)} \, dl + \int\int_{S_{1-3}} f N_i \, dA. \tag{22}$$

Substituting equations (18), (19) and (21) into the weak statement, equation (17), gives

$$\sum_{i,j=1}^{m} H_{ij} \dot{q}_j \delta q_i = \sum_{i=1}^{m} f_i \delta q_i \tag{23a}$$

with

$$H_{ij} = \oint_{L_t} \frac{N_i^{(t)} N_j^{(t)}}{M_t} dl + \int\int_{S_{1-3}} \frac{N_i N_j}{M} dA. \tag{23b}$$

Bear in mind that equation (23a) must hold for any virtual motion δq_i, so that

$$\sum_{j=1}^{m} H_{ij} \dot{q}_j = f_i, \quad i = 1, 2, \ldots, m. \tag{24}$$

It can be seen from equations (22) and (23b) that f_i and H_{ij} depend on the generalized coordinates $\{q_i\}$ nonlinearly but not on the generalized velocities. Therefore, equation (24) is a set of the first-order nonlinear ODEs, which furnishes a dynamic system with the generalized coordinates $\{q_i\}$ to govern the process of the solder profile evolution and the TPL motion driven by surface tensions and gravity.

5. NUMERICAL SIMULATION

5.1. The system of generalized coordinates

To illustrate our modeling, we examine a two-dimensional solder. Figure 3 illustrates the profile of molten solder at a given time during evolution. The solder evolves its profile shape by the specific surface tensions and the gravity field. It is obvious that the mathematical problem corresponding to this solder wetting phenomenon is to evolve a segment of curve in a two-dimensional plane. In fact, we need only consider the segment AB due to the solder's symmetry with respect to the x_2-axis.

Let us describe the segment of curve at a given time t by the position vector $\mathbf{x}$ as the function of a parameter φ, namely

$$\mathbf{x} = \mathbf{x}(\varphi, t). \tag{25}$$

At an arbitrary time, the length of an arc element ds, the unit vector, $\mathbf{n}$, normal to the arc element, and the current curvature of the arc element, κ, can be derived from equation (25). A sign convention adopted here is that the vector $\mathbf{n}$ points from the solder to the gas, and $\kappa > 0$ for a circular solder. The velocity normal to the solder surface is related to the position vector as

$$v_n = \mathbf{n} \cdot \frac{\partial \mathbf{x}}{\partial t} = -\frac{\partial x_2}{\partial s}\frac{\partial x_1}{\partial t} + \frac{\partial x_1}{\partial s}\frac{\partial x_2}{\partial t} \tag{26}$$

where s in equation (26) stands for the arc length measured from Point A toward Point B.

According to the conformal transformation [26], an arbitrary segment of the simple curve that connects Point A and Point B, denoted by C, can be described by the following parametric equations:

$$x_1 = a_{-1} \sin \varphi - \sum_{k=1}^{\infty} a_k \sin(k\varphi) \tag{27a}$$

$$x_2 = a_{-1} \cos \varphi + a_0 + \sum_{k=1}^{\infty} a_k \cos(k\varphi) \tag{27b}$$

where $\varphi \in [0, \varphi_0]$ is a parameter and the coordinates of Points A and B correspond to the values of equations (27) as $\varphi = 0$ and φ_0, respectively. All of

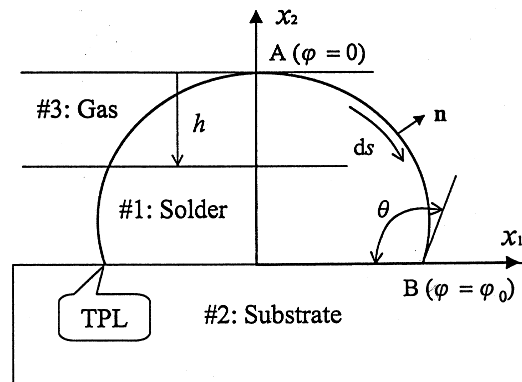

Fig. 3. The profile of a two-dimensional solder at a given time.

the coefficients $\{a_{-1}, a_0, a_1, a_2, \ldots\}$ are real numbers. To meet the requirement that Point B is always on the x_1-axis during the evolution, the constant term a_0 in equation (27b) is chosen as

$$a_0 = -a_{-1}\cos\varphi_0 - \sum_{k=1}^{\infty} a_k \cos(k\varphi_0). \tag{28}$$

Meanwhile, Point A is also on the x_2-axis at any time due to the solder's symmetry with respect to the x_2-axis. Thus equations (27) can be rewritten as

$$x_1 = a_{-1}\sin\varphi - \sum_{k=1}^{m} a_k \sin(k\varphi) \tag{29a}$$

$$x_2 = a_{-1}(\cos\varphi - \cos\varphi_0) + \sum_{k=1}^{m} a_k[\cos(k\varphi) - \cos(k\varphi_0)]. \tag{29b}$$

Here it is noted that we only retain the first m terms of equations (27) in equations (29), so equations (29) will describe the segment C_m, and not segment C. If one takes m sufficiently large, the segment C_m should be as close as possible to the segment C.

From equations (29), we can see that the shape of the segment C, which represents the shape of the solder profile at a given time, is characterized by the coefficients $\{a_i\}$ $(i = -1, 1, 2, \ldots, m)$ as well as φ_0 in the parametric equations (29). Moreover, the coefficients $\{a_i\}$ and φ_0 evolve with time as the solder profile evolves with time. The position vector $\mathbf{x} = \{x_1, x_2\}$ depends on the time with the time implicitly contained in the coefficients $\{a_i(t)\}$ and $\varphi_0(t)$. In the present study, the coefficients $\{a_i, \varphi_0\}$ are chosen as the generalized coordinates of the dynamic system of solder profile evolution to describe the change of the solder shape. The generalized velocities are written as $\{\dot{a}_i, \dot{\varphi}_0\}$, and the degree of freedom of the system is $m + 2$.

5.2. Governing equations

It is obvious that equation (26) can be rewritten as

$$v_n = \left(-\frac{\partial x_2}{\partial\varphi}\frac{\partial x_1}{\partial t} + \frac{\partial x_1}{\partial\varphi}\frac{\partial x_2}{\partial t}\right)\frac{d\varphi}{ds} \tag{30}$$

with the differential relationship between the two arguments s and φ

$$ds = \sqrt{\left(\frac{\partial x_1}{\partial\varphi}\right)^2 + \left(\frac{\partial x_2}{\partial\varphi}\right)^2}\cdot d\varphi. \tag{31}$$

Consequently, substituting equations (29) into equation (30) gives the velocity of the solder surface as

$$v_n = \left(A_{-1}\dot{a}_{-1} + \sum_{k=1}^{m} A_k\dot{a}_k + B_0\dot{\varphi}_0\right)\frac{d\varphi}{ds} \tag{32}$$

with

$$A_{-1} = a_{-1}(1 - \cos\varphi_0\cos\varphi) + \sum_{n=1}^{m} na_n[\cos\varphi_0\cos n\varphi - \cos(n+1)\varphi] \tag{33a}$$

$$A_k = a_{-1}[\cos(k+1)\varphi - \cos k\varphi_0\cos\varphi] + \sum_{n=1}^{m} na_n[\cos k\varphi_0\cos n\varphi - \cos(k-n)\varphi] \tag{33b}$$

$$(k = 1, 2, \ldots, m)$$

$$B_0 = \left(a_{-1}\sin\varphi_0 + \sum_{n=1}^{m} na_n\sin n\varphi_0\right) \times \left(a_{-1}\cos\varphi + \sum_{n=1}^{m} na_n\cos n\varphi\right). \tag{33c}$$

Simultaneously, the velocity of the TPL, that of Point B, is obtained as

$$v_n^{(t)} = \frac{d}{dt}\left(x_1|_{\varphi=\varphi_0}\right) = \sin\varphi_0\dot{a}_{-1} - \sum_{k=1}^{m}\sin(k\varphi_0)\dot{a}_k + \left[a_{-1}\cos\varphi_0 - \sum_{k=1}^{m} ka_k\cos(k\varphi_0)\right]\dot{\varphi}_0. \tag{34}$$

For the sake of convenience, the following equations will be written in dimensionless form. All the variables that have length dimension are normalized by a selected initial length R_0 that measures the initial scale of the solder. For example, let R_0 be the initial radius as the initial shape of the cross-section of the two-dimensional solder is a circle. Meanwhile, all the variables that have the same dimension as the surface tension are normalized by a selected surface tension γ_0. Consequently, the dimensionless generalized coordinates are denoted as

$$\{q_i\} = \{a_{-1}/R_0, a_1/R_0, a_2/R_0, \ldots, a_m/R_0, \varphi_0\} \quad (i = 1, 2, \ldots, m+2) \tag{35}$$

and the dimensionless generalized velocities are written as $\{\dot{q}_i\}$. Thus, the solder surface velocity [equation (32)] is written as

$$v_n = R_0^2\left(\sum_{i=1}^{m+2}\tilde{N}_i\dot{q}_i\right)\frac{d\varphi}{ds} \equiv \sum_{i=1}^{m+2} N_i\dot{q}_i \tag{36}$$

with

$$\{\tilde{N}_i\} = \left\{\frac{A_{-1}}{R_0}, \frac{A_1}{R_0}, \frac{A_2}{R_0}, \ldots, \frac{A_m}{R_0}, \frac{B_0}{R_0^2}\right\} \quad (i = 1, 2, \ldots, m+2) \tag{37}$$

and the TPL velocity [equation (34)] is also written as

$$v_n^{(t)} = R_0\left(\sum_{i=1}^{m+2}\tilde{N}_i^{(t)}\dot{q}_i\right) \equiv \sum_{i=1}^{m+2}N_i^{(t)}\dot{q}_i \tag{38}$$

with

$$\left\{\tilde{N}_i^{(t)}\right\} = \{\sin\varphi_0, -\sin\varphi_0, -\sin 2\varphi_0, \ldots, -\sin m\varphi_0, B_0^{(t)}/R_0\} \tag{39a}$$

$$B_0^{(t)} = a_{-1}\cos\varphi_0 - \sum_{k=1}^{m}ka_k\cos k\varphi_0. \tag{39b}$$

Following Section 4, substituting equations (36) and (38) into equation (24), with the help of equations (22), (23b) and (14), we finally obtain

$$\sum_{i=1}^{m+2}H_{ij}\frac{\mathrm{d}q_i}{\mathrm{d}\tilde{t}} = f_j, \quad j = 1, 2, \ldots, m+2 \tag{40}$$

with

$$H_{ij} = \tilde{N}_i^{(t)}\tilde{N}_j^{(t)} + \chi\int_0^{\varphi_0}\tilde{N}_i\tilde{N}_j\left(\frac{\mathrm{d}\varphi}{\mathrm{d}\tilde{s}}\right)\mathrm{d}\varphi \tag{41a}$$

$$f_j = \left(\frac{\gamma_{2-3}}{\gamma_0} - \frac{\gamma_{1-2}}{\gamma_0} - \frac{\gamma_{1-3}}{\gamma_0}\cos\theta\right)\tilde{N}_j^{(t)} + \int_0^{\varphi_0}\left[\frac{R_0\Delta p}{\gamma_0} - \tilde{\kappa}\frac{\gamma_{1-3}}{\gamma_0}\right]\tilde{N}_j\,\mathrm{d}\varphi. \tag{41b}$$

Here we introduce a dimensionless group χ and a characteristic time t_0 as

$$\chi = \frac{R_0M_t}{M}, \quad t_0 = \frac{R_0}{M_t\gamma_0} \tag{42}$$

and $\tilde{t}$, $\tilde{s}$ and $\tilde{\kappa}$ denote the dimensionless forms of t, s and κ, respectively, such as $\tilde{t} = t/t_0$. In addition, the pressure difference across the solder surface S_{1-3} is expressed as

$$\Delta p = \rho gh + p_0 - p_a \tag{43}$$

where ρg is the specific weight, $h = h(\varphi, t) = x_2(\varphi, t)|_{\varphi=0^\circ} - x_2(\varphi, t)$, measured from the top of the solder, and p_0 and p_a are the internal pressure and the ambient pressure of the molten solder, respectively. Moreover, $p_0 - p_a$ can be determined by the system force balance condition in the x_2-direction as follows:

$$[2x_1(\varphi, t)|_{\varphi=\varphi_0}\cdot\left(p_0 - p_a + \rho gh(\varphi, t)|_{\varphi=\varphi_0}\right) - 2\gamma_{1-3}\sin\theta = \rho gA_0 \tag{44}$$

where A_0 is the area of solder cross-section. The current contact angle θ and curvature κ relate to the generalized coordinates via the following formulae:

$$\cos\theta = \left(\frac{\mathrm{d}x_1}{\mathrm{d}s}\right)\bigg|_{\varphi=\varphi_0}, \quad |\kappa| = \left|\frac{\mathrm{d}\mathbf{x}}{\mathrm{d}\varphi}\times\frac{\mathrm{d}^2\mathbf{x}}{\mathrm{d}\varphi^2}\right|\bigg/\left|\frac{\mathrm{d}\mathbf{x}}{\mathrm{d}\varphi}\right|^3. \tag{45}$$

From equations (40) and (41), it is noted that the set of equations (40) furnishes a nonlinear dynamic system with the generalized coordinates $\{q_i\}$ to govern the solder profile evolution. The solder profile evolution during the solder spreading process depends on the solution of the set of equations (40) under the control parameters: χ, t_0, ρg and γ_{i-j} as well as the initial-value condition

$$q_i(\tilde{t})|_{\tilde{t}=0} = q_{i0}, \quad i = 1, 2, \ldots, m+2 \tag{46}$$

where the initial values $\{q_{i0}\}$ describe the initial shape of the molten solder. In other words, the set of the first-order nonlinear equations (40) with the initial-value conditions (46) governs the solder spreading process.

5.3. *Numerical examples*

Let us consider the following two-dimensional molten solder. The shape of its cross-section at $t = 0$ is

$$\begin{cases} x_1 = r_0\sin\varphi \\ x_2 = r_0[\cos\varphi - \cos\varphi_0(0)] \end{cases}. \tag{47}$$

It is a sector of a circle. r_0 is the radius of the sector of the circle and $\varphi_0(0)$ is the initial value of the generalized coordinate $\varphi_0(t)$. Making a comparison between equations (29) and (47) gives the initial-value condition (46) for the above-mentioned cross-section as

$$\begin{cases} q_1(0) = 1 & q_{m+2} = \varphi_0(0) \\ q_i(0) = 0 & \text{for other } i \end{cases}. \tag{48}$$

It is noted that the initial characteristic length R_0 in equation (35) is selected as the radius r_0. Consequently, under the given initial-value condition (48), the solder evolution depends on the control parameters: χ, t_0, ρg and γ_{i-j}. The Simpson method is adopted to evaluate integrals [equation (41)] and the fourth-order Runge–Kutta method to solve the set of ODEs [equation (40)] for $q_i(t)$. We have performed several case studies to check our

program and to illustrate the phenomena of molten solder profile evolution.

Here we consider the typical case of a lead–tin solder on copper, where the equilibrium contact angle is 15 deg, the surface tension γ_{1-3} is 460 erg/cm^2, and the density of solder material is 8.5 g/cm^3. The initial shape is given by equation (47) with $r_0 = 0.25$ mm, $\varphi_0(0) = 0.9\pi$. The simulation results for $\chi = 1$, 10 and 100 are illustrated by Figs 4–9. Figures 4 and 5 show the traces of the solder shape and the TPL locations at stated times during the evolution process in the case of $\chi = 1$ and 100, respectively.

From Figs 4 and 5, it is clear that the solder shape change and TPL motion are extremely rapid at the beginning of spreading in shorter time, then followed by a slow spreading process in longer time before reaching static equilibrium shape. The comparison between Figs 4 and 5 shows that the time duration to reach the static equilibrium state (denoted by t_e) for a small dimensionless parameter χ, is shorter than that for large χ. This conclusion can also be drawn from Figs 6–8. Actually, the normalized equilibrium times, t_e/t_0, are estimated in the above numerical examples and they are 70, 130 and 550 for $\chi = 1$, 10 and 100, respectively. As expected, the final static equilibrium solder shapes are the same as for all three cases and it is the same as the computed solder equilibrium shape using Laplace–Young equations [4]. Moreover, we can predict not only the equilibrium shape of the solder, but also the shape at any time during the spreading process.

Figure 6 shows the dependence of contact angle on the time, Fig. 7 shows the dependence of the normalized spreading area, $A/R_0^2 = (x_1/R_0)|_{\varphi=\varphi_0}$,

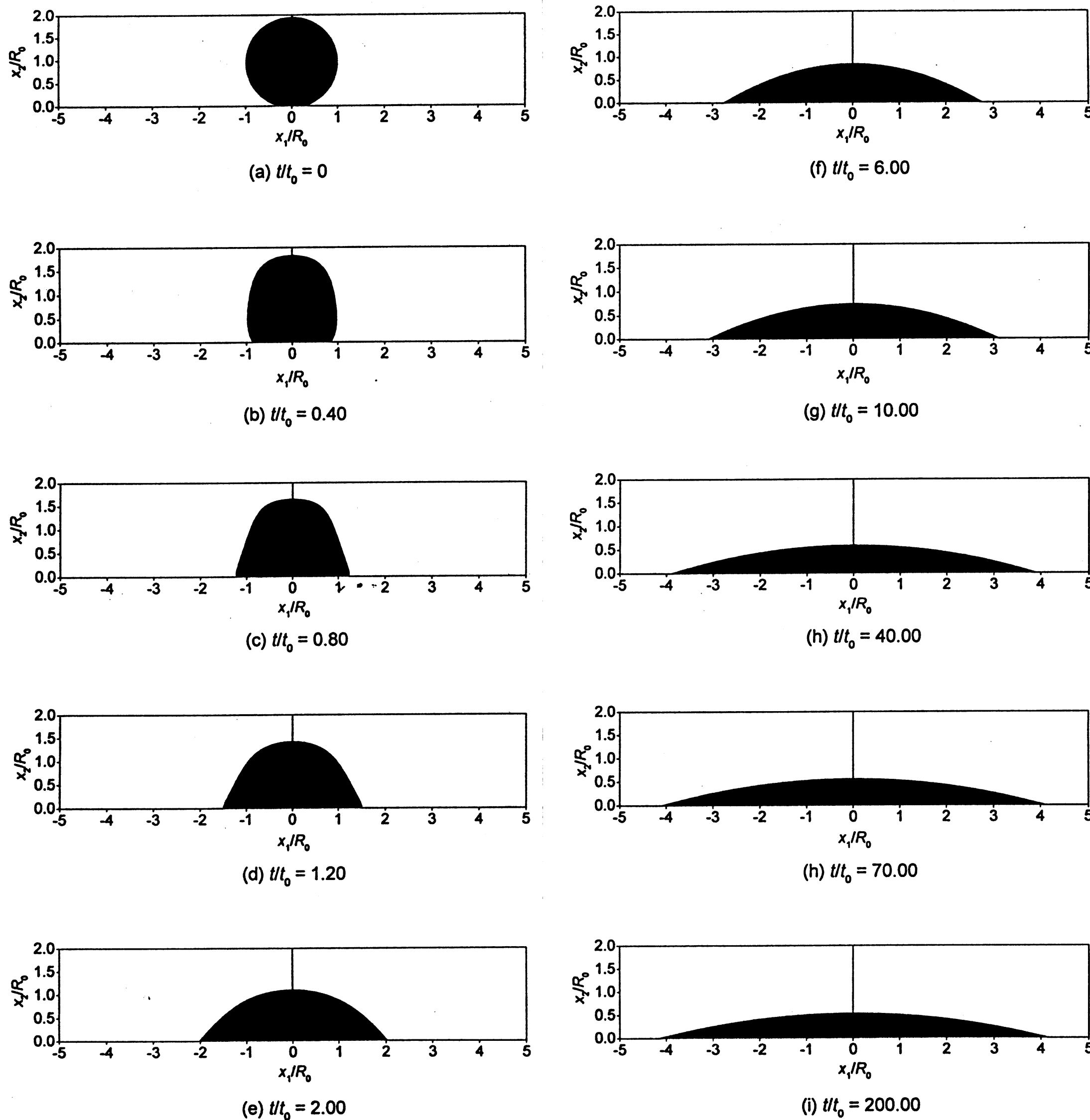

Fig. 4. The traces of the solder shape at the stated times ($\chi = 1$).

(a) $t/t_0 = 0$

(b) $t/t_0 = 5.00$

(c) $t/t_0 = 10.00$

(d) $t/t_0 = 14.00$

(e) $t/t_0 = 15.00$

(f) $t/t_0 = 30.00$

(g) $t/t_0 = 70.00$

(h) $t/t_0 = 200.00$

(h) $t/t_0 = 550.00$

(i) $t/t_0 = 900.00$

Fig. 5. The traces of the solder shape at the stated times ($\chi = 100$).

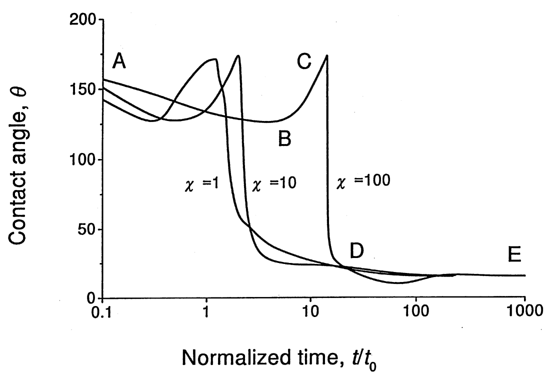

Fig. 6. The dependence of the contact angle (θ) on time (t/t_0).

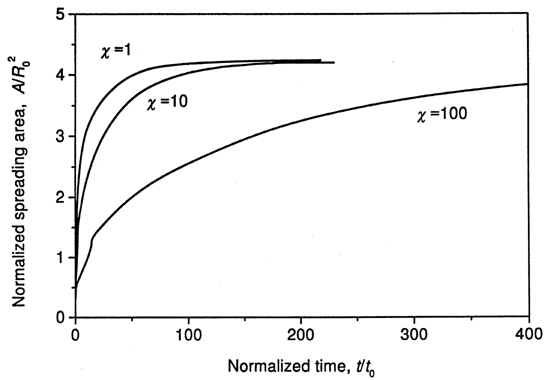

Fig. 7. The dependence of the spreading area (A/R_0^2) on time (t/t_0).

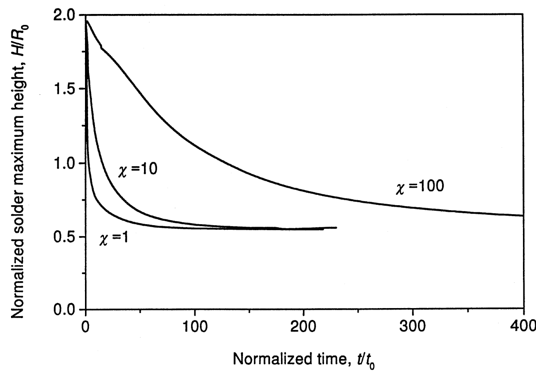

Fig. 8. The dependence of the solder maximum height (H/R_0) on time (t/t_0).

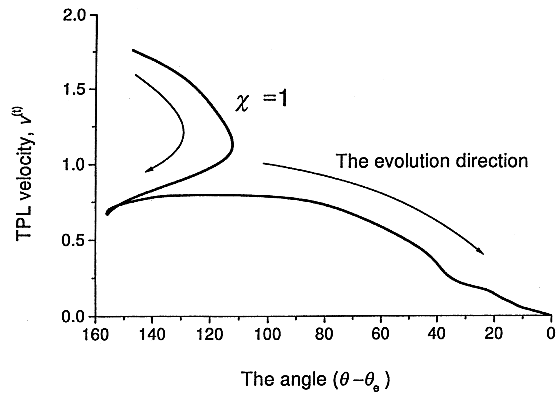

Fig. 9. The relation between the TPL velocity ($v^{(t)}$) on the angle ($\theta - \theta_e$).

on time, and Fig. 8 shows the solder maximum height, $H = x_2|_{\varphi=0}$, on time, respectively.

Figure 6 shows that the process that the current contact angle changes with time experiences four stages. It decreases rapidly and reaches a valley point (Point B) at the first stage (from A to B), then climbs to a peak in a short time at the second stage (from B to C), the peak is higher then the start point A. At the third stage (from C to D), it experiences an extremely rapid drop, then followed by a slow change at the fourth stage (from D to E) in a long time before it reaches the equilibrium contact angle. The maximum solder height and the spreading area, as illustrated in Figs 7 and 8, are two easily measurable parameters in the experiments.

6. SUMMARY AND DISCUSSION

A better understanding of solder alloy wetting and spreading is expected to be important for soldering in microelectronics, where the sizes of devices are very small and sound solderabilities are required. This paper presents a theoretical model to describe solder wetting and spreading in its molten state. The time-dependent processes of solder profiles evolution and triple point lines motion driven by surface tensions and gravity can be modeled by a nonlinear dynamic system. It leads to a set of nonlinear ODEs with generalized coordinates. The numerical procedure and examples for the solution of the dynamic system have been described.

The numerical simulation includes the time sequences of solder profiles and the changes of the contact angles, the maximum solder height and the spreading areas with time. They show that the solder spreading process first experiences an extremely rapid spreading and is then followed by a slow spreading before at last reaching static equilibrium shape. It is in agreement with experimental observation [9]. Our model can be applied to predict not only the equilibrium shape of the solder, but also the shape at any time during the spreading process.

In the fluid mechanics models (see, e.g. Ref. [14]) for solder spreading, it is assumed

$$v^{(t)} = K(\theta - \theta_e)^n \tag{49}$$

for the TPL kinetics, where $v^{(t)}$ is the velocity of the TPL, and K and n are constants. This equation is not obtained from the basic principles of fluid mechanics, rather an assumption. Inconsistency of assumption (49) and experimental observation has been reported in Refs [11, 13]. From the present model, we can derive the relation between $v^{(t)}$ and $(\theta - \theta_e)$. Actually, the combination of Figs 6 and 7 gives the relation illustrated by Fig. 9.

The $v^{(t)}$ vs θ relation mainly depends on the two material constants: M and M_t in the kinetics laws (11). These two mobilities are introduced in terms of the scheme of dynamics system, and to be determined by comparing model predictions with experimental observations. Further three-dimensional calculations with the real material constants and shape parameters used in experiments are required to clarify the present model quantitatively. It is also hoped that experiments will succeed in ascertaining the significance of the process in real solder wetting.

REFERENCES

1. Hampshire, B. and Wolverton, M., in *The Mechanics of Solder Alloy Wetting and Spreading*, ed. F. G. Yost, F. M. Hosking and D. R. Frear. Van Nostrand Reinhold, New York, 1993, p. 9.
2. Heinrich, S. M., in *The Mechanics of Solder Alloy Interconnects*, ed. D. Frear, H. Morgan, S. Burchett and J. Lau. Van Nostrand Reinhold, New York, 1994, p. 158.
3. Heinrich, S. M. and Lee, P. S., in *Advances in Electronic Packaging*, EEP-Vol. 19-2, 1997, p. 1371.
4. Finn, R., *Equilibrium Capillary Surface*. Springer-Verlag, New York, 1986.
5. Li, Y. and Mahajan, R. L., *Trans. A.S.M.E. J. Electron. Packaging*, 1998, **120**, 118.
6. Chiang, K.-N. and Chen, W.-L., *Trans. A.S.M.E. J. Electron. Packaging*, 1998, **120**, 175.

7. Brakke, K. A., *Surface Evolver Manual, Version 2.10*. The Geometry Center, University of Minnesota, Minneapolis, 1998.
8. Renken, F. P. and Subbarayan, G., *Trans. A.S.M.E. J. Electron. Packaging*, 1998, **120**, 302.
9. Yost, F. G., Hosking, F. M. and Frear, D. R., in *The Mechanics of Solder Alloy Wetting and Spreading*, ed. F. G. Yost, F. M. Hosking and D. R. Frear. Van Nostrand Reinhold, New York, 1993, p. 1.
10. Whalley, D. C. and Conway, P. P., *Trans. A.S.M.E. J. Electron. Packaging*, 1996, **118**, 134.
11. Moon, K. W., Boettinger, W. J., Williams, M. E., Josell, D., Murray, B. T., Carter, W. C. and Handwerker, C. A., *Trans. A.S.M.E. J. Electron. Packaging*, 1996, **118**, 174.
12. Yost, F. G., Hosking, F. M. and Frear, D. R., *The Mechanics of Solder Alloy Wetting and Spreading*. Van Nostrand Reinhold, New York, 1993.
13. Boettinger, W. J., Handwerker, C. A. and Kattner, U. R., in *The Mechanics of Solder Alloy Wetting and Spreading*, ed. F. G. Yost, F. M. Hosking and D. R. Frear. Van Nostrand Reinhold, New York, 1993, p. 103.
14. Ehrhard, P. and Davis, S. H., *J. Fluid Mech.*, 1991, **229**, 365.
15. Aksay, I. A., Hoge, C. A. and Pask, J. A., *J. phys. Chem.*, 1974, **78**, 1178.
16. Mortensen, A., Drevet, B. and Eustathopoulos, N., *Scripta mater.*, 1997, **36**(6), 645.
17. Mortensen, A., Hodaj, F. and Eustathopoulos, N., *Scripta mater.*, 1998, **38**(9), 1411.
18. Voitovitch, B., Mortensen, A., Hodaj, F. and Eustathopoulos, N., *Acta mater.*, 1999, **47**(4), 1117.
19. Wang, G. and Lannutti, J. J., *Metall. Mater. Trans. A*, 1995, **26A**, 1499.
20. Yost, F. G., Sackinger, P. A. and O'Toole, E. J., *Acta mater.*, 1998, **46**(7), 2329.
21. Warren, J. A., Boettinger, W. J. and Roosen, A. R., *Acta mater.*, 1998, **46**(9), 3247.
22. Yost, F. G., *Scripta mater.*, 1998, **38**(8), 1225.
23. Yost, F. G. and O'Toole, E. J., *Acta mater.*, 1998, **46**(14), 5143.
24. Suo, Z., *Adv. Mech.*, 1997, **33**, 193.
25. Yang, W. and Suo, Z., *Acta mech. sin. (English Series)*, 1996, **12**(2), 144.
26. Muskhelishvili, N. I., *Some Basic Problems of the Mathematical Theory of Elasticity*. Noordhoff, Leyden, The Netherlands, 1975, (translated from Russian by J. R. M. Radok).